Cyclic Loading in Hypoplastic Facial Sutures: Can it Enhance Growth?

Dong (David) Uk Shin

A thesis

submitted in partial fulfillment of the

requirements for the degree of

Master of Science in Dentistry

University of Washington

2020

Committee:

Susan W. Herring

Katherine Rafferty

Tracy Popowics

Zee (Zi-Jun) Liu

Program Authorized to Offer Degree:

Orthodontics

University of Washington

Abstract

Cyclic Loading in Hypoplastic Facial Sutures: Can it Enhance Growth?

Dong (David) Uk Shin

Chair of the Supervisory Committee:
Professor Susan W. Herring
Orthodontics and Oral Health Sciences

Introduction: Midfacial deficiency is one of the contributors to Class III malocclusions. Severe cases of this skeletal disharmony can be functionally debilitating, cause severe airway issues including sleep apnea, and be disfiguring in form. Many treatments have been proposed, including surgery. A less invasive alternative would be mechanical modulation of the suture, allowing for changes in growth, and overall changes in the craniofacial complex. Static forces are used in orthodontics routinely, but cyclic forces, especially in dentofacial orthopedics, have not been thoroughly studied. Previous studies using cyclic loading on normal animals have suggested positive effects, but whether the treatment would work on midface deficient animals is unknown. Cyclically loaded sutures were hypothesized to be wider, more vascular, and to have less organized collagen fibers than sham sutures.

Methods: Yucatan minipigs, which are naturally midface-deficient, were treated with a protocol for cyclic loading or sham loading (n=6/group) of the right nasofrontal suture (RNFS). After euthanasia, suture samples with fluorescent bone markers were embedded in

plastic and sectioned. The right and left nasofrontal suture and right coronal suture were of interest. 4x images were combined and a histomorphometric analysis of the sutural width and calcein bone apposition width was completed. Additional samples were decalcified and embedded in paraffin. Sections were stained with a lectin protocol to measure endothelial cell density and with Sirius Red to describe collagen organization.

Results: The Yucatan minipigs showed no statistically significant difference in sutural width and mineral apposition between experimental and sham sutures. The targeted right nasofrontal suture tended to be narrower in the experimental minipigs, opposite to the expected result. Endothelial cell density was similar in comparing the central zones of experimental vs sham control groups, and all sutures showed a tendency for the central zone to be denser than the osteogenic zone. Sirius Red staining suggested few differences, but some experimental nasofrontal sutures had more disorganized collagen fibers throughout the suture compared to the sham controls, which had more uniform fibers, usually obliquely oriented.

Conclusions: The results are not indicative that treatment will increase sutural width or increase vascularity although collagen organization may be affected. Abnormally growing sutures may be insensitive to cyclic loading or incapable of responding to it because of other constraints.

Table of Contents

Introduction

Midfacial hypoplasia manifests as a Class III dental malocclusion in 5-15% of the population (Ngan 2010). Midfacial hypoplasia suggests that nasomaxillary sutures have not grown in relation to the rest of the craniofacial complex. Severe cases of midfacial hypoplasia can be functionally debilitating, cause severe airway issues, including sleep apnea, and be disfiguring in form. Craniofacial sutures should not ossify before growth is completed, and must be patent to allow intramembranous bone apposition to facilitate growth of the cranial bones (Opperman 2000). However, in non-syndromic midfacial hypoplasia, the sutures are not overtly fused, yet they are clearly not growing at the normal rate. Underdevelopment of these key sutures that should grow in harmony with the mandible can not only be esthetically unpleasing, but functionally harmful as well.

Midfacial deficiency and underdevelopment can occur in isolation, or in conjunction with various other disorders (Kreiborg 2000, Marchac et al. 2012). To address this deficiency, many treatment alternatives have been proposed, including surgery. A less invasive alternative would be mechanical modulation of the suture, allowing for changes in growth, and overall changes in the craniofacial complex. Static forces on sutures are used in dentofacial orthopedics, including reverse-pull headgears (Kopher and Mao 2003). According to these authors, continuous static forces have not been shown to be the optimal treatment for sutural growth (Mao 2002). Instead, they advocated intermittent cyclic forces to induce increases in the width of the sutures and subsequent osteogenesis. The effects of static sutural loading have been studied as well. Different types of headgears have been studied on *Macaca* monkeys. Specifically, *Macaca mulatta*

monkeys have been subjected to static compressive forces through a high-pull headgear, resulting in retardation of maxillary growth (Meldrum 1975), whereas facemask headgears incorporating static tensile forces in *Macaca nemestrina* monkeys have been shown to increase anterior maxillary displacement (Jackson et al., 1979). In human clinical trials of distraction osteogenesis in patients with craniofacial deformities, it is without doubt that the use of static forces has restored function and esthetics. However, two studies have curiously reported early and late relapse (Al-Daghreer et al. 2008, Marchac and Arnaud 2012).

The more recent treatment alternative proposed was cyclic loading. The theoretical advantages include brief/daily treatment regimens rather than full-time wear, and the possibility that compressive as well as tensile loads could enhance growth. Cyclic loading induced greater bone formation and increase in sutural width in comparison to static loading in a rabbit study (Kopher and Mao 2003). There have also been data that suggest that no matter what the type of loading (compressive or tensile), sutural width and osteogenesis are increased (Peptan et al. 2008). These studies in the past on cyclic forces all suggest that this force may be more effective than static loading. However, the animal models here were rats and rabbits and the loading regime required clamping the head in a materials testing machine. Until recently, a study on larger mammals (which may more accurately translate to the human model) had not been done. Perhaps in humans, cyclic forces would be more efficient on a patient wearing a loading apparatus half an hour a day, versus wearing a facemask for 12+ hours.

A pilot study on the pig model to investigate cyclic loading of the nasofrontal suture assessed the distribution of strain and the resulting growth at various suture sites (Soh et al. 2018). Ordinary farm pigs (*Sus scrofa domesticus*) without midfacial deficiencies were chosen for this study. The nasofrontal suture was the primary focus. Growth at this suture directly lengthens the midface, as the suture lies in between the cranium and nasal complex (Popowics and Herring 2007). The nasofrontal suture also mineralizes rapidly, corresponding with the fast growth of this region in pigs (Rafferty and Herring 1999). A portable loading device was developed. The study suggested that daily cyclic loading modified and increased strain in the skull, and that five days of loading sufficed to increase growth at the nasofrontal suture, with a mean increase in mineral apposition rate of 18 μm/day. Thus, daily cyclic loading in short intervals may be a more efficient growth modification method than static loading for midfacial deficiencies. Based on these findings, this thesis will focus on addressing these short daily cyclic forces on the nasofrontal suture in hypoplastic sutures of midface deficient pigs, specifically the Yucatan minipig. Yucatan minipigs were chosen as they have midface deficiency and crowding of the upper dentition (Fig. 1). The objective was to establish whether cyclic loading can help sutures that are growing poorly.

Yucatan craniofacial sutures differ from those of farm pigs. The nasofrontal suture was reported to have more active osteoblasts on the bone fronts compared to farm pigs (Rafferty et al. 2019). This is interesting as it could allude to the cause of midface deficiency, as more active osteoblasts would result in more bone formation and earlier fusion of the sutural space. Possibly with cyclic loading, these four month old Yucatan

minipigs can respond favorably to mechanical load, as the sutures have not fused and cyclic loading caused similar strains in both the farm and Yucatan minipigs (Rafferty et al. 2019).

The central zone of sutures differs from the osteogenic zones of the sutures. The central zone is thought to be more vascular and collagen fibers are more interwoven and less aligned than near the bone edges (Sun et al. 2007). The central zone also contains undifferentiated cells, at least in young mice (Zhao et al. 2015). These stem cells may allow for increased vascularization in sutures in response to mechanical stresses (Zhao et al. 2015). The orientation of collagen fibers typically resists sutural deformation. For instance, the bone front regions of the compressed nasofrontal suture have collagen oriented to resist the force. However, the more random orientation of the central zone (Popowics et al. 2007) may render the vessels vulnerable to mechanical loading and lead to a hypoxic environment. In normal rat sutures collagen structure changes with load applied, with the amount of Type I collagen increasing, and Type III collagen introduced as well (Tanaka et al. 2000).

We speculate that cyclic loading causes a disturbance in the blood flow of the central zone sutural tissues. This mechanical disruption, which itself might widen the sutural gap by breaking down connective tissue, may lead to an environment of hypoxia, which tends to keep cells in an undifferentiated state. A hypoxic environment would lead to an upregulation of angiogenic expression in the central zone of the sutures, which would then lead to increased angiogenesis while not inhibiting osteogenesis at the bone fronts

(Lana-Elola 2007; Sun et. al 2007). Thus, this thesis hypothesizes an increase in the amount of centrally located endothelial cells after cyclic loading. In hypoxia a mechanosensor, Periostin, is upregulated, which increases matrix turnover (Linder et al. 2005; Yoshiba et al. 2007). Cyclic loads may prevent collagen from maturing into organized ligaments by requiring continuous matrix remodeling. Therefore, another expectation is to find irregular collagen organization and a lack of collagen density in the middle third of sutures. If these expectations are correct, these signs should be seen in any treated suture, whether normal or hypoplastic. Thus, this study will assess the notion that cyclic loading could alter vascularity and collagen content in the central zone, while simultaneously promoting sutural separation and growth at the bone fronts.

The significance of this study is its potential for understanding how sutures react to cyclic loads and its translational value for developing clinical treatments for midfacial hypoplasia. Future studies and alternative therapies may surface, such as angiogenic mediators that may be administered in midface deficient subjects. The rationale for this research is the possibility that growth in midfacial hypoplastic patients could be altered by cyclic loading, providing a novel treatment alternative for the orthodontist.

Therefore the objectives of this study are first, to assess whether there is any effect of cyclic loading on sutural growth in animals with midfacial hypoplasia, measured as the width of the sutural space and mineral apposition, and second, to understand the changes in the vascular and collagen content in both normal and hypoplastic sutures. Our hypothesis of mechanism proposes that the effect is mediated at the central zone of

sutures through increases in the vasculature and decreases in collagen organization. To assess whether this hypothesis is correct and to fulfill the objectives listed above, the specific aims are:

1. Measure the width of the sutural space and amount of mineral apposition at the bone fronts in Yucatan minipigs and to compare cyclically loaded animals with sham controls.
2. In both farm pigs and Yucatan minipigs, compare loaded and sham loaded sutures in terms of:
    a. Endothelial cell content
        i. Assess whether the central zone is more vascular than osteogenic zones in sutures generally.
        ii. Ascertain the effect of cyclic loading on vasculature of loaded vs sham controls, specifically whether loading alters total vascularity or ratio of osteogenic zone to central zone vascularity.
    b. Amount and organization of collagen

Materials and Methods

Apparatus and Procedures

Yucatan minipigs of both sexes, 4 months old, were obtained in same-sex pairs from S+S Farms (Brentwood, CA), n=6 pairs. A sample size of 6 per group was previously determined based on a power analysis. One member of each pair was treated with cyclic loading; the other was a sham control. Material from the pilot study (Soh et al. 2018) on farm pigs (n=3 treated, n=1 sham) supplemented the endothelial and collagen sample. All experimental procedures were approved by the University of Washington Institutional Animal Care and Use Committee. Fig. 1 illustrates a typical Yucatan skull of this age. All individuals showed midfacial hypoplasia, albeit of varying degree.

Cyclic or sham forces were applied to the right nasofrontal suture (RNFS) (Fig. 1) via plates with 2 cm projecting rods which had been surgically placed into the right frontal and nasal bones (Fig. 2). After healing for one week, the pigs were assigned randomly to the cyclic loading or sham group. For five days daily, the pigs were anesthetized and positioned prone. The loading device engaged the projections. In the loaded group a cycling tensile force (except in pig 934 where a compressive force was mistakenly placed) was applied via a voice coil and a sine wave electrical current that moved the central rod at the masticatory rate of 2.5 Hz (Fig. 2). Masticatory strain of the nasofrontal suture is compressive (Herring 1993). Loaded animals received 4500 cycles a day over 30 minutes, with 22,500 cycles over 5 days. In the sham group, the device engaged the rods but was set at 0 and thus did not provide any cyclic loading. The pigs then were returned to their pens. Fluorochrome labels for mineral apposition was administered IV

on days 1 (calcein, SIGMA; 12.5 mg/Kg in sterile saline filtered using a 0.22 μm Millex Syringe-driven Filter Unit) and 3 (alizarin complexone, SIGMA; 12.5 mg/Kg in sterile saline delivered similarly) of loading. On day 5, after the final loading session, animals were killed while anesthetized, and preservative injected through the vascular system. Blocks containing the sutures and about 5 mm of surrounding tissue were removed from the skull. Specimen were stored in 70% alcohol. Each suture block was then bisected, with one part left undecalcified (plastic-embedded) for evaluation of the width and mineral apposition at the suture site. The other part was decalcified, paraffin-embedded, and sectioned at 5-7 μm for endothelial and collagen staining. Although all six pairs of pigs had undecalcified slides available for measurement, only five pairs of pigs had decalcified sections prepared.

Analysis of Sutural Width and Apposition

The undecalcified samples were immersed in a mixture of 4% formaldehyde, 1% glutaraldehyde in 0.1M sodium cacodylate buffer (pH 7.4, prepared from 0.2M sodium cacodylate buffer, Electron Microscopy Sciences, Hatfield, PA). Then they were washed three times in 0.2M sodium cacodylate buffer, dehydrated in a graded ethanol series (70%, 90%, 100%), and infiltrated with 3 changes of 100% Micro-bed resin (Electron Microscopy Sciences, Hatfield, PA). Finally, the samples were infiltrated with fresh resin overnight. The samples then underwent curing at 35-36 °C in an oven. After curing for roughly 21 days, the samples were sectioned perpendicular to the sutures at 50 μm thickness using a saw microtome (Leica SP1600). Sections were mounted on slides with Cytoseal 60 (No. 8310-4, Richard-Allan Scientific, Thermo Fisher Scientific Inc).

For aim 1, these sections were examined under epifluorescent illumination (Nikon Eclipse E400; Nikon Y-FL, Japan) for measurement of the average sutural width and mineral apposition at the bone fronts. The fields of calcein and alizarin were captured under green and red fluorescent light using a digital camera (SPOT RT3 2Mp Slider, Diagnostic Instruments, Inc, Sterling Heights, MI) and MetaVue software (Universal Imaging Corp, Downingtown, PA). Image Composite Editor software (Microsoft Corporation, Redmond, WA) was then used to stitch together the different series of separate images in the field of interest (Fig. 3). Unfortunately, the alizarin fluorescence was not bright enough to visualize clearly, so only the calcein label could be measured. MetaMorph (Molecular Devices, LLC, San Jose, CA) was used for linear calibrations and histomorphometric analysis. The sutural margins were traced and the area between them was measured and divided by the average length of the two margins to give average sutural width (Fig. 3). For day 1 of mineral apposition, the brightly fluorescent areas of calcein near the bone fronts were traced to calculate the area of new mineral deposition (Fig. 3). Selection of slides and measurements were performed by two investigators (D.S. and K.S.) who were blinded to the treatment groups and identity of any sutures.

Inter-investigator measurement error was assessed by re-measuring 10 random samples a few months after the original measurements. The Dahlberg formula ($\sum(d2/2n)1/2$) was used to calculate the method error. For statistical analysis, paired t-tests and two-sample t-tests were conducted in Excel to test hypotheses and explore the data. Comparisons were made between the right and left nasofrontal sutures of the animal and between the sutures of experimental and sham control animals.

Analysis of Endothelial Cell Density and Collagen Organization

Lectin, a glycoprotein that binds to vascular endothelial carbohydrates, was used to detect endothelial cells (Minamikawa et al. 1987). After preparation of the sections with Avidin/Biotin Blocking Kit (Vector Labs SP-2001, Burlingame, CA), the samples were incubated with hydrogen peroxide (2%). Afterwards, the sections were exposed to unconjugated *Griffonia Simplicifolia* lectin I (Vector Labs B-1105, Burlingame, CA) overnight. Mouse IgG negative controls were similarly done. The sections were then incubated with VECTASTAIN ABC Peroxidase (Vector Labs PK-6100, Burlingame, CA). Afterwards, the sections were treated with ImmPACT DAB Peroxidase HRP Substrate (Vector Labs SK-4105, Burlingame, CA). Finally, the sections were counter-stained with hematoxylin, dehydrated and cover slipped with Cytoseal 60 medium (Richard-Allan Scientific, Kalamazoo, MI).

All measurements were made by the same investigator (D.S.), who remained blinded to treatment and suture identity. Images of the stained sections were captured at 10x using MetaVue and merged (Fig. 4). Then dorsal, middle, and ventral locations were geometrically defined and used for analysis. These images were imported into Photoshop. The suture width was divided into thirds: the two osteogenic zones and the central zone. The method utilized the line tool in Photoshop and is shown in Fig. 5. Then the color threshold tool in Photoshop was used to select the brown stained pixels (lectin-stained endothelial cells) using an average threshold of 45 for variation in staining. This resulted in uniform green pixels that were then used to calculate endothelial density (Fig. 6) in each third of the suture, by selecting each area manually and overlaying a black fill to

isolate the area of interest (Fig. 7). The images were then transferred to the MetaMorph program for quantification. The overall area of the entire image was calibrated at 10x magnification and found to be 1715 μm x 1280 μm, or a total area of 2.195mm squared. Each area was separately calculated in the MetaMorph program. Endothelial cell density was then determined by dividing the total area of the thresholded pixels (Fig. 7) by the total area of the site of interest that was determined. This was done separately for each osteogenic zone and the central zone. The two osteogenic zones for each suture were averaged, as well as the dorsal, middle, and ventral images of the suture, to arrive at the final averaged osteogenic and central zone values.

For assessing collagen in the sutural space, slides were stained with Sirius Red (Sindelar et al. 2002) and visualized with polarized light (Fig. 8). The Abcam Picro-Sirius Red Stain Kit (Ab150681, Cambridge, UK) was used following the manufacturer's protocol. Dorsal, middle, and ventral images were selected at 10x as before. Due to the complexity of collagen organization, a descriptive approach was adopted. Although the investigator (D.S.) was blinded to treatment, experimental-sham pairs could be identified by ID number. These pairs were compared for differences in subjective collagen appearance. Five categories were set for descriptions of each section: 1) general impressions of collagen orientation: parallel vs oblique, 2) bony attachment points and angle, 3) classification of dense vs sparse fibers, 4) number of bony interdigitations 5) wide vs narrow sutural space.

Intra-investigator measurement error for endothelial cell density was assessed by re-

measuring 10 random samples a few months after the original measurements. The Dahlberg formula ($\sum(d2/2n)1/2$) was used to calculate the method error. For statistical analysis, paired t-tests and two-sample t-tests were conducted in Excel. Because of small sample size, non-parametric Mann-Whitney U tests were also used, but results were similar for ratio comparisons, which are not normally distributed, only Mann-Whitney U tests were performed. Comparisons between right and left nasofrontal sutures and between sham and control were performed separately for Yucatans and the farm pigs from the previous study. Yucatan and farm pig experimental groups were also compared.

Results

It should be noted again that one experimental pig, labelled 934 E/R, had been loaded in reverse. However, it is included in the calculations because (1) polarity is not thought to matter for cyclic loading, and (2) its data fall into the range of the other animals.
Suture widths are shown in Table 1. Measurement error was low for sutural width calculations (5.5%), but only fair for calcein label (18%). The lower repeatability of calcein measurement was likely due to the subjective nature of selecting brightest area of fluorescence.

Table 1 and Figure 9 show that for both the experimental and sham groups, the right (targeted) and left sides of the nasofrontal suture were similar in width ($p=0.35$) suggesting no local effect of the right-side loading in the experimental group. In fact, in 4 of the 6 experimental Yucatans, the targeted right side was actually narrower than the left side.

Comparing the right nasofrontal suture for experimental vs sham indicated that the sham suture was actually wider (161.4 μm, experimental vs 223.9 μm, sham, $p=0.048$). However, no experimental vs sham differences were seen for the left nasofrontal suture ($p=0.32$) or the right coronal suture ($p=0.36$). Interestingly, however, the coronal sutures are clearly much narrower than the nasofrontal sutures regardless of side or group (86-96 μm vs 161-224 μm, Table 1).

Mineral Apposition

Table 2 and Fig. 10 show that uptake of the calcein varied among animals, complicating the comparison of averages. Nevertheless, neither parametric nor nonparametric statistics indicate any difference between right and left nasofrontal sutures, nor between experimental and control sutures. Similar to the width measurements, coronal suture calcein deposition was much less than that of the nasofrontal sutures (28-34 μm vs 114-136 μm, Table 2).

Endothelial Cell Density Measurements

The measurement error for endothelial density measurements was 2.5%, which indicates that the method that was developed was reliable and repeatable. Using the color threshold tool in Photoshop eliminated bias, and calculating the density was largely uniform across samples. The small remaining error was likely from dividing the suture into equal thirds, which can change depending on where the line is drawn on the captured image.

Table 3 and Fig. 11 show the data for the endothelial cell density. Lectin-stained area ranged from 0.5-2.7% of total area. It is notable that vascularity was generally greater in Yucatan minipigs than in farm pigs in all regions. The central zones were usually more vascular than the osteogenic zones, but not always significantly so (Fig. 11). Since there were no differences between groups, the data were combined (experimental + sham) for a sample size of 10 and a paired t-test was conducted and the central zone was significantly more vascular than the osteogenic zone (Table 3). The data also suggest that unlike sutural width and mineral apposition, vascularity of the coronal suture was similar to that

of the nasofrontal suture. Furthermore, there is no evidence of an effect of cyclic loading on vascularity of either the central or osteogenic zone, nor the ratio of the two zones.

Collagen organization comparisons

The dorsal, middle, and ventral images of each suture were examined, but no distinct trends were noted. Comparison of experimental and sham pairs did yield differences in some cases (Table 4). It should be noted that although the load was applied to the right nasofrontal suture, the left nasofrontal suture received similar albeit lower cyclic loads. The right coronal suture yielded no trends or notable differences between slides and across experimental and sham animals.

For the one pair of farm pigs, 594 (experimental), and 595 (sham), the targeted right nasofrontal suture of the experimental pig had generally sparser fibers than that of the sham 595 (Fig. 12). However, sparseness did not characterize the targeted right nasofrontal suture in any of the Yucatan minipigs. In fact, one pair (7900/7910) showed denser fibers in the experimental 7900. However, fiber direction sometimes seemed disrupted in experimental sutures, specifically in pig 934's right nasofrontal suture (as compared to 938, Fig. 13) and 3351 left nasofrontal suture (as compared to 3355, Fig. 14). Tears in the central zone were noted in two experimental and two sham pigs and so were not likely due to loading.

Discussion

Limitations and Considerations

This experiment used an arbitrary loading regime, but one which appeared to enhance sutural separation and growth in small animals (Kopher and Mao 2003) and had encouraging results in a pilot study on farm pigs (Soh et al. 2018). The apparatus did not offer a pure translational load to the suture because the location of the loading device outside of the skull inevitably caused some bending. It is possible that certain areas of the suture such as the dorsal aspect, were less tensed than the ventral aspect or even compressed. In addition to a small sample size, some of the data collection was subjective, and the quantitative measurements of mineral apposition were less repeatable than desired. Moreover, the failure of the second fluorescent label (alizarin), prevented an accurate measure of mineral apposition rate, and it is not clear what significance should be attached to deposition of calcein on day 1 of loading.

The mistake of loading Yucatan minipig 934 in reverse is a further limitation. The reversed load placed the nasofrontal sutures under compression and tensed the right coronal suture, opposite to the rest of the experimental pigs. However, the overall results should not be affected, as tension or compression should produce the same results in cyclic loading.

The small sample size was exacerbated by sectioning and staining problems. With those problems, pigs 5045/5049 were not usable for Sirius red and lectin.

Description of collagen amount and organization proved very subjective and difficult in this complex three dimensional sutural space.

Consideration must also be made that the focus and actual test of the hypothesis was for the right nasofrontal suture as the loading was applied there. However, the other sutures were explored as there was indirect loading that was transmitted to the other sutures of interest.

Sutural Width

Disappointingly, the treatment did not enhance the sutural space. There were no strong statistical differences in any measure. The original hypothesis was that the experimental right nasofrontal suture would have the widest sutural width, as this is the suture that received direct cyclic loading from our apparatus. It was also hypothesized that all experimental sutures would have increased sutural width compared to the sham controls. Not only were these hypotheses not supported, but the targeted right nasofrontal suture tended to be narrower, not wider, in experimental Yucatans compared to shams (161 μm, SD 27.5 μm vs. 223 μm, SD 62.3 μm respectively, $p=0.048$). A similar but smaller trend was seen when the less loaded left nasofrontal sutures were compared (Table 1). This finding conflicts not only with the previous literature on rabbits and rats (Kopher and Mao 2003), but also with our own small pilot study on farm pigs (Soh et al. 2018), all of which suggested that cyclically loaded sutures are widened.

It is, of course, possible that the farm pig pilot study findings were statistical artifact, as sample size was only 3 experimental and 1 sham. Alternatively, the present study is the first to test sutures in animals with midfacial hypoplasia. The sutures of Yucatans do differ from those of other pigs; they are simpler, narrower, more cellular in osteogenic zones, and have less well organized sutural ligaments (Rafferty et al. 2019). Even though cyclic loading of Yucatan vs farm pig sutures produced similar strains (Rafferty et al. 2019), the Yucatan sutures may have been incapable of responding, either because they are mechanically insensitive or because they are prevented from expanding by restriction from other parts of the skull. We speculate that the latter is the case, because the narrower widths in the loaded nasofrontal sutures imply an osteogenic response at the bone fronts—bone lengthening without a comparable increase in sutural space available. This situation might actually hasten the fusion of loaded sutures, an undesirable result. It is also possible that these Yucatan pigs may have a midface deficiency due to other reasons we are not aware of, such as nasal septum deficiency, causing the treatment to fail.

The present study also confirms the previous finding that the coronal suture is narrower than the nasofrontal suture. Regardless of whether the section was in the experimental or the sham group, this difference was very clear. Sutural width has often been implicated with growth, with wider sutures implying more growth potential and increased growth rate as a result (Opperman 2000). Possibly, these narrower coronal sutures are growing more slowly and will undergo synostosis earlier than the nasofrontal sutures.

Calcein Mineral Apposition

Calcein width was a measure of mineral apposition that occurred on the first day of loading. Given this limited scope, the less-than-ideal repeatability of the measure, and the variability among pigs, it is not surprising that no significant loading effect was found. Because previous research with cyclic loading has suggested an increase in mineral apposition (Soh et al. 2018), it was hypothesized that calcein widths would be greater with the experimental treatment in comparison to the sham control. This would also explain the narrowing of the nasofrontal sutures in the loaded Yucatan minipigs since sutural space did not increase. There was indeed a slight difference in this direction, but it was far from statistically significant. Because of the technical problems with this procedure, it was not a definitive measure of apposition, so it remains a possibility that cyclic loading could increase growth of the bone fronts even in hypoplastic sutures. If so, however, given the absence of space expansion, the effect might hasten suture fusion and would be counterproductive as a treatment.

Endothelial Cell Density

The rationale for examining vascularity was that cyclic loading would disrupt blow flow, causing a hypoxic environment that would be angiogenic and help preserve patency of the central zone. Thus the loading regime was expected to increase vascularity, particularly in the central zone. Endothelial density in the central zone was similar in loaded and sham right nasofrontal sutures, the targeted suture. There was a trend for the ratio of osteogenic: central zone endothelial density to be greater in the loaded right nasofrontal suture, but it was far from statistical significance and was not supported by

data from farm pigs. Thus the rationale is likely incorrect. As sutural vascularity has rarely been the subject of investigation, however, more data are needed. Although there did not appear to be a treatment effect, there did appear to be a breed difference, Yucatan sutures generally had higher endothelial density than the farm pig sutures. This suggests that the abnormal sutures of the Yucatan minipigs are more vascular than normal sutures in farm pigs, perhaps corresponding with the increased cellularity noted previously (Rafferty et al. 2019). However, we cannot eliminate the possibility that the immunohistochemistry might have worked less well in the farm pig slides because those slides had been stored longer.

Finally, the results confirm the subjective impression that the central zone of sutures is more vascular than the osteogenic zone generally. There was a trend for the right nasofrontal suture central zone to have greater endothelial staining than the osteogenic zone, and this was further supported when the Yucatan data were combined (experimental + sham) for a sample size of 10. Farm pigs showed a similar tendency for higher endothelial content in the central zone than in the osteogenic zone.

Collagen Organization

Collagen organization was found to be extremely complex and variable in these 3-dimensional sutures. Thus, it is difficult to identify any conclusive trends. The expectation for collagen disorganization and decreased density in the central zone was not consistently seen, although a few of the loaded nasofrontal sutures appeared to show a loss of fiber orientation especially in the central zone. Cyclic loading may or may not

have an effect on collagen density as originally hypothesized, but it must be remembered that only five days of loading occurred, and there may not have been enough time for adaptation. The occasional appearance of tears in the central zone was not a treatment effect, as tears were seen in both experimental and sham groups. Thus, they probably were artifacts from histological preparation, or possibly from the original surgery, since the tears were always on the right side, where the posts had been implanted.

Conclusions

In contrast to results achieved with normally growing animals, cyclic loading of Yucatan minipigs with midfacial hypoplasia produced no statistically significant increase of sutural width or mineral apposition. Indeed, there was a tendency for narrowing of the targeted suture. Similarly, cyclic loading did not significantly alter endothelial content of sutures. However, the central zone of the sutures was found to be more vascular than the osteogenic zones, and the sutures of hypoplastic Yucatan minipigs were generally more vascular than those of normal farm pigs. Some loaded sutures indicated loss of collagen alignment, but this was not a consistent finding. The inability of hypoplastic sutures to expand under loading suggests that they are restrained by other structures in the skull, perhaps slow-growing or early-mineralizing cranial base cartilages.

Acknowledgments

I would like to thank the following for their invaluable help throughout this research: my committee (Susan W. Herring, Katherine Rafferty, Tracy Popowics, Zee (Zi-Jun) Liu) for their development and guidance throughout, Kelsey Smith for her work and help throughout this project, Jay Park for her help in taking images of the undecalcified sections, Josh Dizon and Edwin Lee for their many hours in histological work. A special thank you to Tracy Popowics for her invaluable help in the histological staining protocols. And of course, an enormous thank you to Katherine Rafferty for her guidance and support, and my mentor Susan Herring who has always supported and offered help at a moment's notice.

I would also like to thank the University of Washington Orthodontic Alumni Association and NIDCR #R21DE024814 for funding this project.

Bibliography

Al-Daghreer S, Flores-Mir C, El-Bialy T. 2008. Long-term stability after craniofacial distraction osteogenesis. J Oral Maxillofac Surg. 66(9):1812-9.

Herring, S.W., Z.F. Muhl, and A. Obrez 1993. Bone growth and periosteal migration control masseter muscle orientation in pigs (Sus scrofa). Anat. Rec., 235: p. 215-222.

Jackson GW, Kokich VG, Shapiro PA. 1979. Experimental and postexperimental response to anteriorly directed extraoral force in young Macaca nemestrina. Am J Orthod. 75(3):318-33.

Kopher RA, Mao JJ. 2003. Suture growth modulated by the oscillatory component of micromechanical strain. J Bone Miner Res. 18(3):521-8.

Kreiborg, S., 2000. Postnatal growth and development of the craniofacial complex in premature craniosynostosis, in Craniosynostosis, M.M.J. Cohen, Editor. Oxford Univ. Press: New York. p. 158-174.

Lana-Elola, E., et al. 2007. Cell fate specification during calvarial bone and suture development. Dev Biol, 311(2): p. 335-46.

Lindner, V., et al. 2005. Vascular injury induces expression of periostin: implications for vascular cell differentiation and migration. Arterioscler Thromb Vasc Biol, 25(1): p. 77-83.

Mao JJ. 2002. Mechanobiology of craniofacial sutures. J Dent Res. 81(12):810-6.

Mao JJ, Wang X, Mooney MP, Kopher RA, Nudera JA. 2003. Strain induced osteogenesis of the craniofacial suture upon controlled delivery of low-frequency cyclic forces. Front Biosci. 8:a10-7.

Marchac, A. and E. Arnaud. 2012. Cranium and midface distraction osteogenesis: current practices, controversies, and future applications. J Craniofac Surg. 23: p. 235-238.

Meldrum RJ. 1975. Alterations in the upper facial growth of Macaca mulatta resulting from high-pull headgear. Am J Orthod. 67(4):393-411.

Minamikawa, T., T. Miyake, T. Takamatsu and S. Fujita. 1987. A new method of lectin histochemistry for the study of brain angiogenesis. Lectin angiography. Histochemistry 87(4): 317-20.

Ngan, P. and H. He. 2010. Effective maxillary protraction for Class III patients, in Current Therapy in Orthodontics, R. Nanda and S. Kapila, Editors. Mosby/Elsevier: St. Louis. p. 143-158.

Opperman LA. 2000. Cranial sutures as intramembranous bone growth sites. Dev Dyn. 219(4):472-85.

Peptan AI, Lopez A, Kopher RA, Mao JJ. 2008. Responses of intramembranous bone and sutures upon in vivo cyclic tensile and compressive loading. Bone. 42(2):432-8.

Popowics TE, Herring SW. 2007. Load transmission in the nasofrontal suture of the pig, Sus scrofa. J Biomech. 40(4):837-44.

Rafferty KL, Baldwin MC, Soh SH, Herring SW. 2019. Mechanobiology of bone and suture – Results from a pig model. Orthod Craniofac Research. 22(Suppl. 1): 82-89.

Rafferty KL, Herring SW. 1999. Craniofacial sutures: morphology, growth, and in vivo masticatory strains. J Morphol. 242(2):167-79.

Sindelar, B.J., S. Edwards, and S.W. Herring. 2002. Morphologic changes in the TMJ following splint wear. Anat Rec. 266: p. 167-176.

Self, C. 2015. Tooth Roots and the Periodontal Ligament: Morphology, Modeling and Behavior. Unpublished Doctor of Philosphy dissertation, University of Washington, Seattle, Washington.

Soh, S, Rafferty K, Herring S, 2018. Cyclic Loading Effects on Craniofacial Strain and Sutural Growth in Pigs. Am J Orthod. 154(2):270-282.

Sun, Z. 2007. Angiogenesis of a Mandibular Distraction Osteogenesis Site and its Relationship to Masticatory Strain. Bone. 41(2): 188–196.

Sun, Z., E. Lee, and S.W. Herring. 2007. Cell proliferation and osteogenic differentiation of growing pig cranial sutures. J Anat. 211: p. 280-289.

Tanaka, E., et al. 2000. Effects of tensile forces on the expression of type III collagen in rat interparietal suture. Arch Oral Biol. 45(12): 1049-1057.

Yoshiba, N., et al. 2007. Association of TIMP-2 with extracellular matrix exposed to mechanical stress and its co-distribution with periostin during mouse mandible development. Cell Tissue Res. 330: p. 133-145.

Zhao, H., et al. 2015. The suture provides a niche for mesenchymal stem cells of craniofacial bones. Nature Cell Biol. 17: p. 386-396.

Tables and Figures

Table 1: Summary of Yucatan Minipig Sutural Widths (μm).

	Experimental	Experimental	Experimental
	Right Nasofrontal Suture	Left Nasofrontal Suture	Right Coronal Suture
Pig 934	149	155	71
Pig 1517	158	231	74
Pig 2581	141	165	103
Pig 3351	182	136	99
Pig 5049	132	163	123
Pig 7900	205	175	106
Final Average	**161**	**171**	**96**
Standard Deviation	**28**	**32**	**20**

	Sham	Sham	Sham
	Right Nasofrontal Suture	Left Nasofrontal Suture	Right Coronal Suture
Pig 938	194	194	77
Pig 1518	199	162	66
Pig 2598	159	171	78
Pig 3355	188	152	95
Pig 5045	296	335	101
Pig 7910	309	202	102
Final Average	**224**	**203**	**86**
Standard Deviation	**62**	**68**	**15**

Paired t-test	Experimental	Sham
Nasofrontal Suture	p=0.61	p=0.35

2 sample t-test	Right Side	Left Side
Nasofrontal Suture	p=0.05	p=0.32
Right Coronal Suture	p=0.36	NA

Table 2: Summary of Yucatan Minipig Calcein Widths (μm)

	Experimental	Experimental	Experimental
	Right Nasofrontal Suture	Left Nasofrontal Suture	Right Coronal Suture
Pig 934	165	152	28
Pig 1517	157	224	59
Pig 2581	212	303	62
Pig 3351	29	41	15
Pig 5049	66	57	31
Pig 7900	64	37	10
Final Average	**116**	**136**	**34**
Standard Deviation	**72**	**110**	**22**

	Sham	Sham	Sham
	Right Nasofrontal Suture	Left Nasofrontal Suture	Right Coronal Suture
Pig 938	106	181	11
Pig 1518	192	175	27
Pig 2598	106	115	44
Pig 3355	55	34	22
Pig 5045	122	110	48
Pig 7910	102	74	17
Final Average	**114**	**115**	**28**
Standard Deviation	**44**	**57**	**15**

Paired t-test	Experimental	Sham
Nasofrontal Suture	p=0.35	p=0.95

2 sample t-test	Right Side	Left Side
Nasofrontal Suture	p=0.96	p=0.69
Right Coronal Suture	p=0.59	NA

Table 3: Endothelial Areal Density (%) of Yucatan and Farm pigs.

	Right Nasofrontal Suture	Right Nasofrontal Suture	Right Nasofrontal Suture	Left Nasofrontal Suture	Left Nasofrontal Suture	Left Nasofrontal Suture	Right Coronal Suture	Right Coronal Suture	Right Coronal Suture
Yucatan Experimental	**Osteogenic Zone**	**Central Zone**	**Osteogenic/ Central Ratiox100**	**Osteogenic Zone**	**Central Zone**	**Osteogenic/ Central Ratiox100**	**Osteogenic Zone**	**Central Zone**	**Osteogenic/ Central Ratiox100**
Pig 934	0.8	1.0	82	0.9	2.5	38	0.7	1.7	44
Pig 1517	0.3	1.8	16	1.4	2.5	54	0.8	0.9	80
Pig 2581	0.4	0.5	81	1.1	0.9	123	0.4	0.8	46
Pig 3351	0.9	1.6	64	0.7	0.2	302	No Sections	No Sections	No Sections
Pig 7900	0.8	1.9	42	0.5	0.6	82	1.3	1.8	71
Final Average	*0.7*	*1.4*	*57*	*0.9*	*1.3*	*120*	*0.8*	*1.3*	*60*
Standard Deviation	*0.3*	*0.6*	*28*	*0.3*	*1.1*	*106*	*0.4*	*0.5*	*18*
Yucatan Sham									
Pig 938	1.3	1.1	112	0.4	1.5	29	1.0	1.4	74
Pig 1518	1.2	1.5	79	1.1	1.2	96	0.2	0.5	31
Pig 2598	1.1	2.6	44	2.0	2.2	91	2.7	2.3	117
Pig 3355	0.6	0.7	79	0.4	0.6	65	NA	NA	NA
Pig 7910	0.8	1.2	67	0.4	1.0	37	0.6	1.0	57
Final Average	*0.9*	*1.4*	*76*	*0.9*	*1.3*	*63*	*1.1*	*1.3*	*69*
Standard Deviation	*0.3*	*0.7*	*24*	*0.7*	*0.6*	*30*	*1.1*	*0.7*	*36*

Table 3 cont.

	Right Nasofrontal Suture	Right Nasofrontal Suture	Right Nasofrontal Suture	Left Nasofrontal Suture	Left Nasofrontal Suture	Left Nasofrontal Suture	Right Coronal Suture	Right Coronal Suture	Right Coronal Suture
Farm Experimental	**Osteogenic Zone**	**Central Zone**	**Osteogenic/ Central Ratiox100**	**Osteogenic Zone**	**Central Zone**	**Osteogenic/ Central Ratiox100**	**Osteogenic Zone**	**Central Zone**	**Osteogenic/ Central Ratiox100**
Pig 594	0.4	0.6	59	0.3	0.5	70	0.3	0.8	31
Pig 414	0.2	0.5	41	0.3	0.3	82	0.4	0.7	61
Pig 57	0.4	0.5	79	0.4	0.6	67	0.3	0.7	45
Final Average	*0.3*	*0.5*	*60*	*0.3*	*0.5*	*73*	*0.3*	*0.7*	*46*
Standard Deviation	*0.1*	*0.1*	*19*	*0.1*	*0.2*	*8*	*0.1*	*0.1*	*15*
Farm Sham									
Pig 595	0.5	0.9	56	0.6	1	60	No Sections	No Sections	No Sections

Table 3 cont. *

Paired t-test	Experimental	Sham
Yucatan RNFS Osteogenic Zone vs Central Zone	p=0.06	p=0.17
Yucatan RCS Osteogenic Zone vs Central Zone	p=0.05	p=0.38
Farm RNFS Osteogenic Zone vs Central Zone	p=0.01	NA
Farm RCS Osteogenic Zone vs Central Zone	p=0.04	NA

Paired t-test	
Yucatan RNFS Experimental+Sham Osteogenic Zone vs Yucatan RNFS Experimental + Sham Central Zone	p=0.01

2 sample t-test	Right Side
Yucatan Experimental vs Sham NFS Central Zone	p=0.92
Yucatan Experimental vs Farm Experimental NFS Central Zone	p=0.06
Yucatan Experimental vs Farm Experimental NFS Osteogenic Zone	p=0.09

Ratios

Mann-Whitney U test	Right Side	Left Side
Yucatan Experimental vs Sham NFS Osteogenic:Central Zone Ratio	p=0.28	p=0.28
Yucatan Experimental vs Sham RCS Osteogenic:Central Zone Ratio	p=0.67	NA
Yucatan Experimental NFS vs Farm Experimental NFS Osteogenic:Central Zone Ratio	p=0.88	p=0.49
Yucatan Experimental RCS vs Farm Experimental RCS Osteogenic:Central Zone Ratio	p=0.30	NA

* Right Nasofrontal Suture (RNFS), Left Nasofrontal Suture (LNFS), Right Coronal Suture (RCS)

Table 4: Collagen organization comparisons between experimental/sham pairs.

	Experimental	Experimental
	Right Nasofrontal Suture	Left Nasofrontal Suture
Pig 594	Sparse fibers in central zone	Similar to sham
Pig 934	Disorganized fibers, with different orientation in each third of the suture. More attachment points, 25, all close to 45 degrees.	Similar to sham
Pig 1517	Similar to sham	Similar to sham
Pig 2581	Tear visible on one slide	Similar to sham
Pig 3351	Similar to sham	No clear pattern, difficult to distinguish fiber orientation. Dorsal aspect of central zone has striations that appear to be blood vessels
Pig 7900	Dense fibers	Similar to sham

	Sham	Sham
	Right Nasofrontal Suture	Left Nasofrontal Suture
Pig 595	Dense fibers in central zone	Similar to right side
Pig 938	Uniform oblique fiber orientation across the suture 5-8 attachment points, roughly 70-90 degrees	Similar to right side
Pig 1518	Tears in the central zone Roughly parallel fiber orientation throughout the suture	Similar to right side but no tear
Pig 2598	No tears	Similar to right side
Pig 3355	Tear visible on one slide Parallel, uniform fibers throughout the suture	Similar to right side but no tear
Pig 7910	Uniform fiber orientation	Similar to right side

Figure 1: Yucatan minipig skull with labeled sutures.

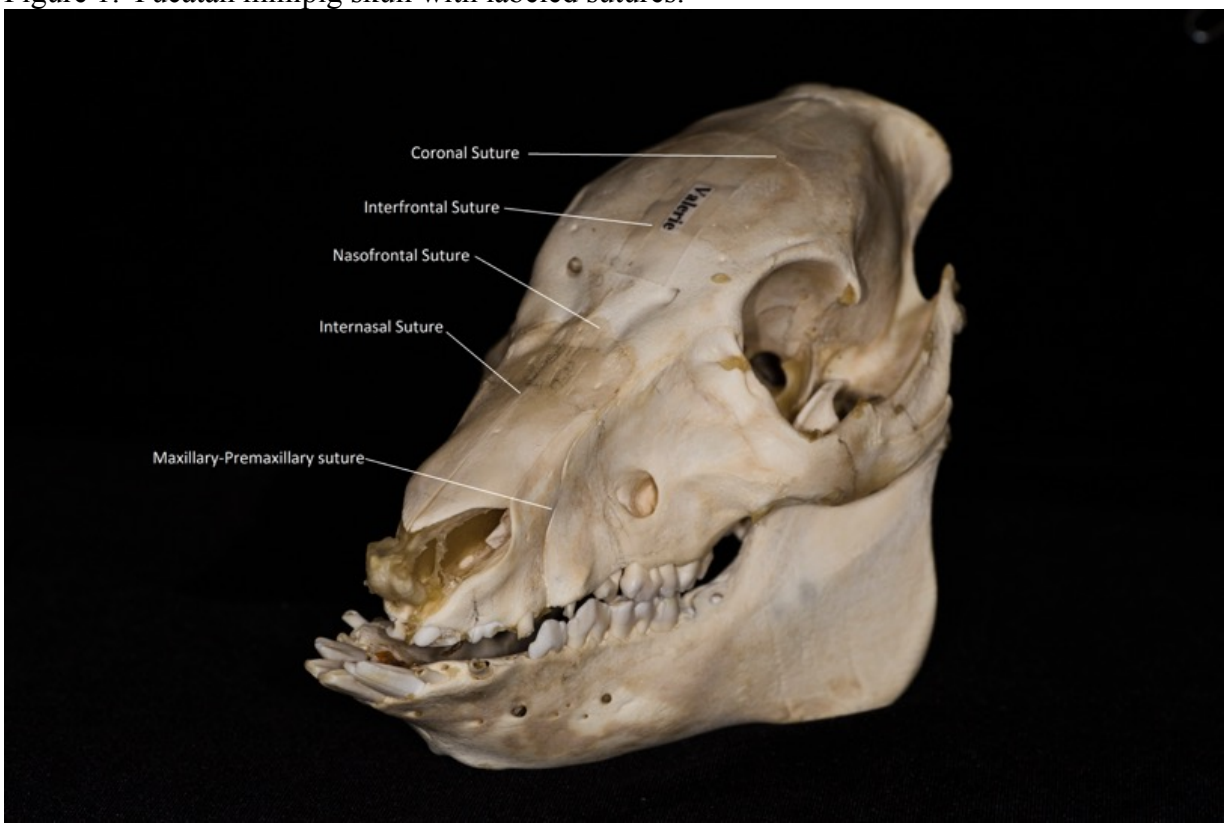

Figure 2: Illustration of the motorized loading device. The voice coil (VC) houses a magnet that moves a rod in response to an electrical current. The load cell (L) measures force applied.

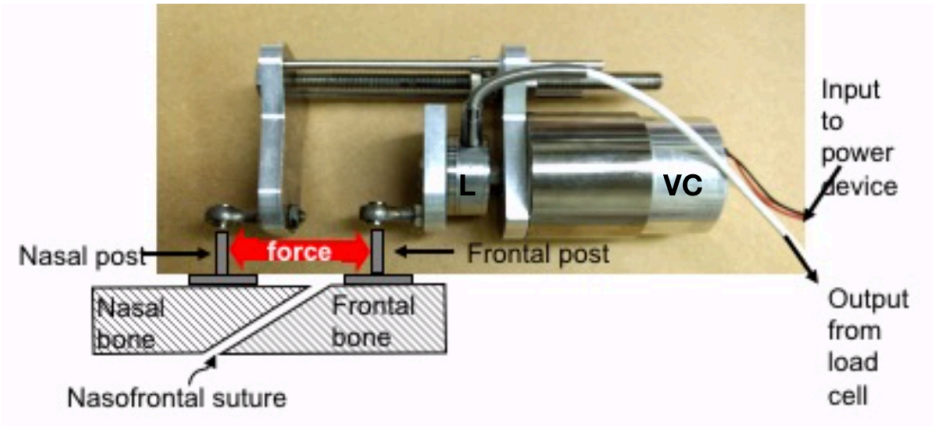

Figure 3: A. Right nasofrontal suture of Yucatan minipig 1517, images taken at 4x and merged. Calcein shows as green, Alizarin is red, but was too faint for quantification. B. The sutural space was filled in (yellow). C. Calcein-labeled areas were false-colored (pink).

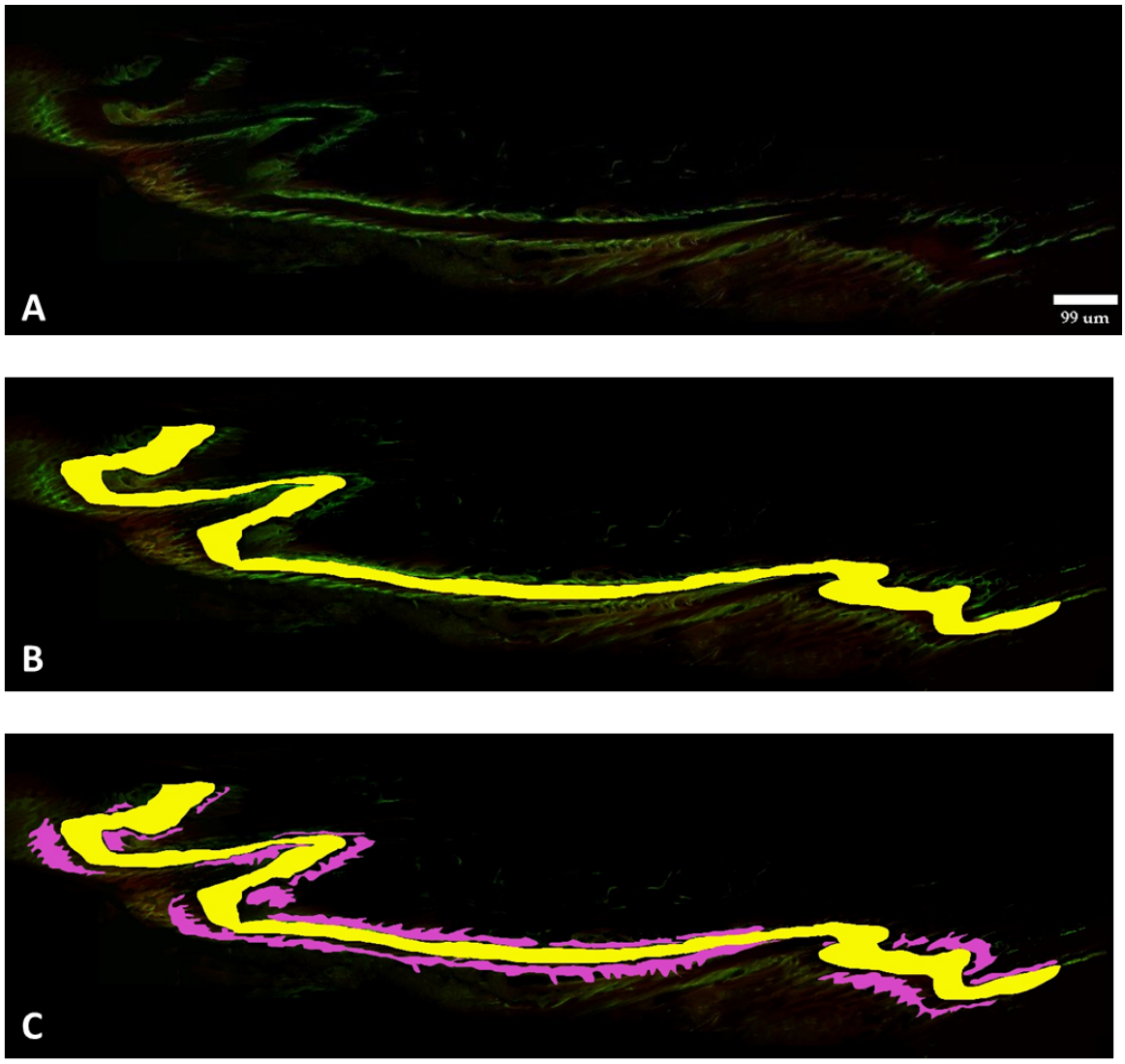

Figure 4: Merged lectin stained sutures with 10x individual pictures of a right nasofrontal suture of Yucatan minipig 1518. Dorsal, middle, and ventral areas of interest are shown in black boxes. Calibration bar 500 μm.

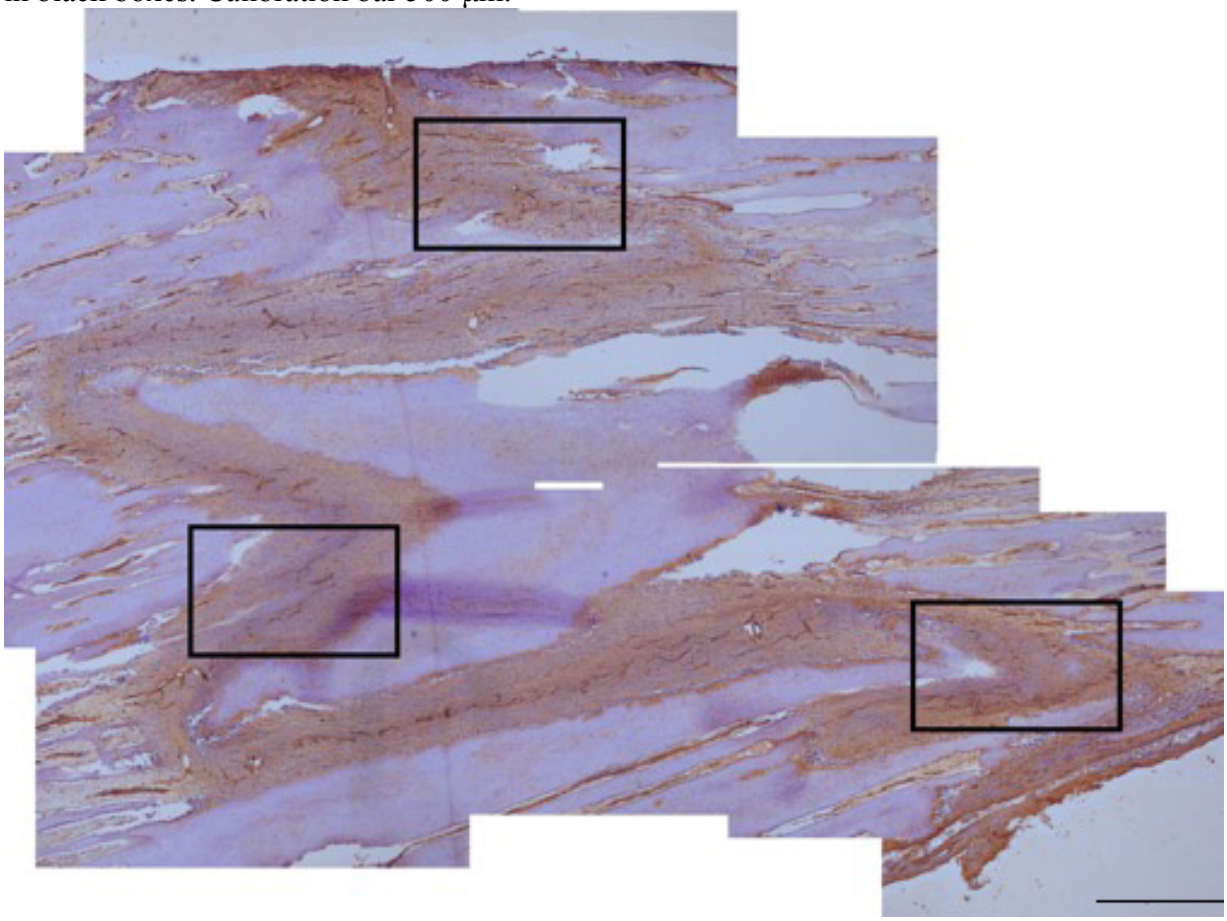

Figure 5: Image of dorsal black box in Figure 4. The line tool of Photoshop measured the distance from the bony front to the other bony front, which was divided by 3. The 6-8 lines were then connected by a final line which defined the 2 osteogenic zones and the central zone. Lectin-stained endothelial cells are dark brown. Calibration bar 500 μm.

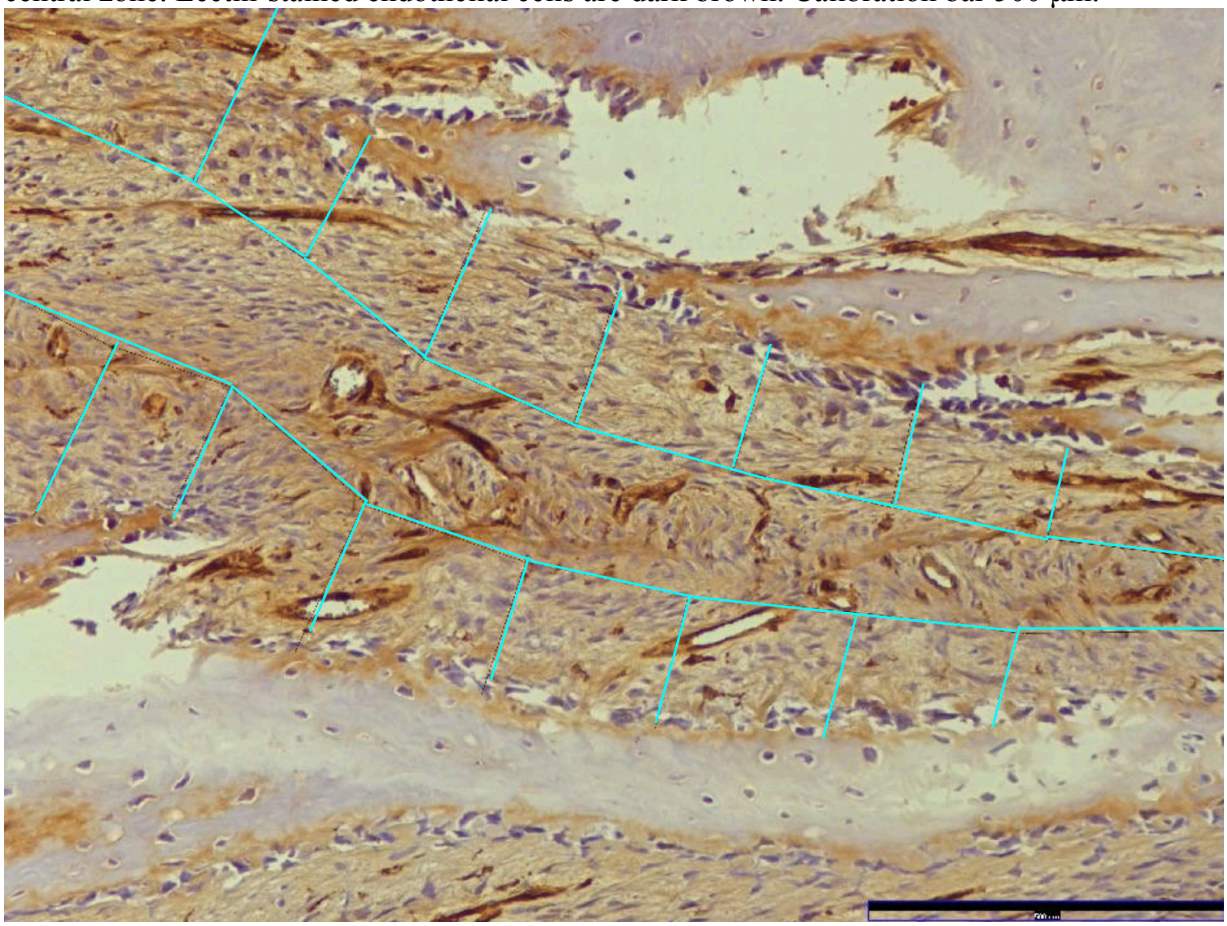

Figure 6: Color thresholded endothelial content of the previous image (Fig. 5).
Calibration bar 500 µm.

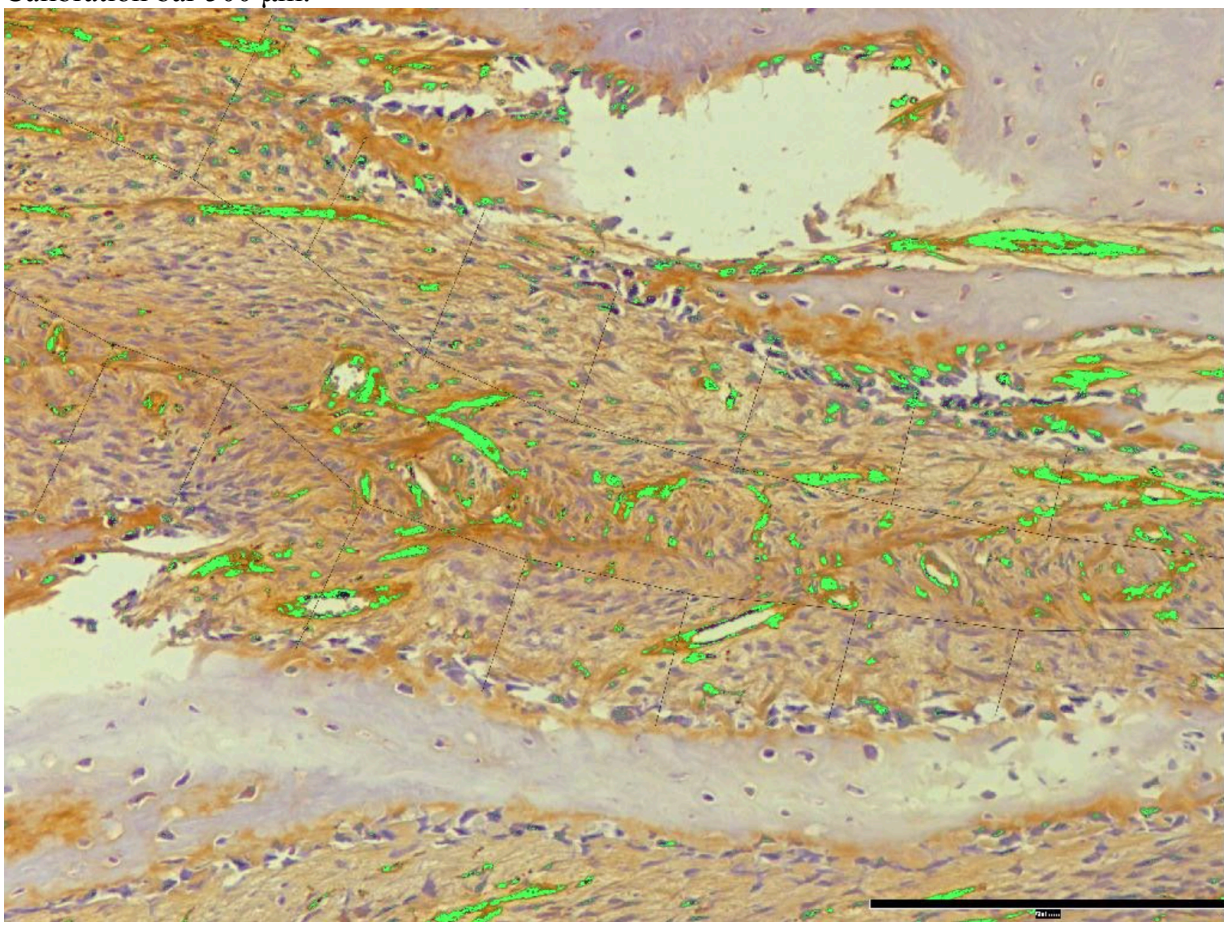

Figure 7: Isolation of each third of the suture in (Fig. 6) by selecting each area manually and overlaying a black fill to isolate. Nasal bone osteogenic zone, central zone, and frontal bone osteogenic zone (A, B, C respectively). Calibration bar 500 μm.

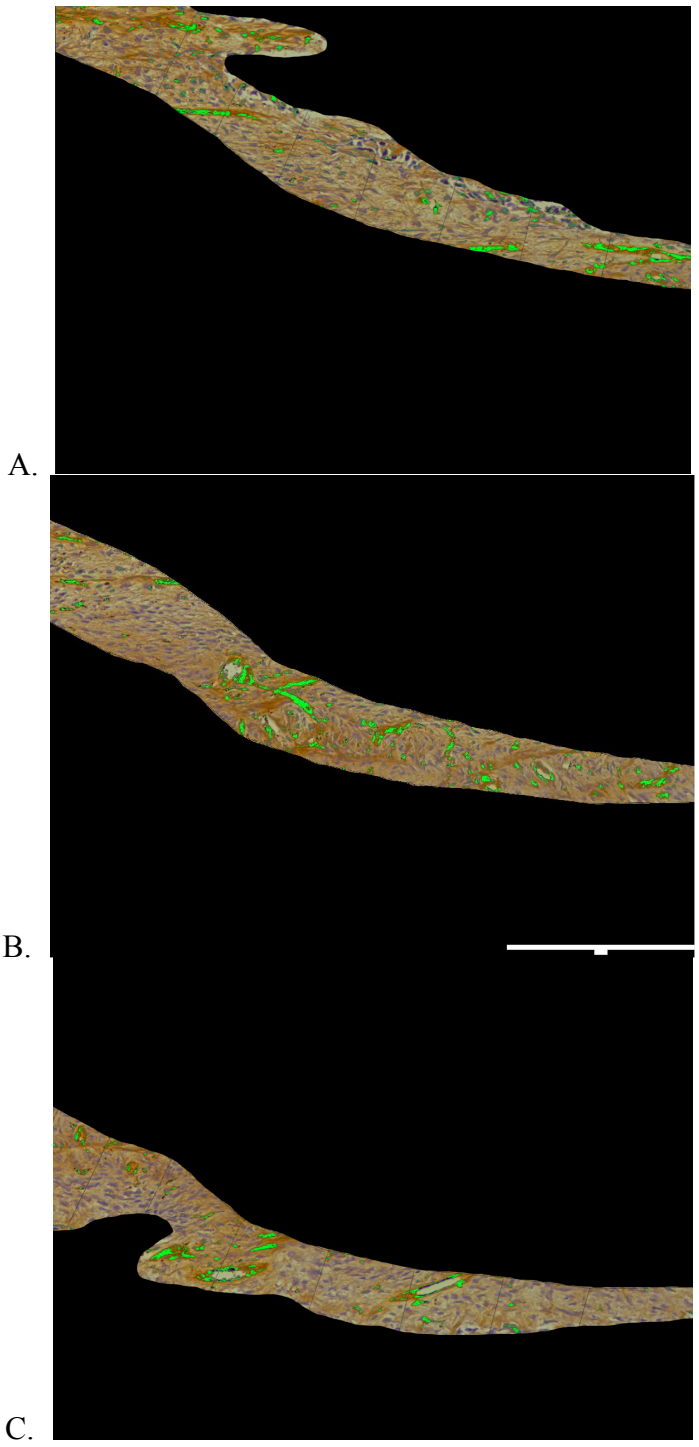

Figure 8: Right nasofrontal suture of farm pig 595 (sham) stained with Sirius red for collagen. Bright field image (above) and polarized image (below), 10x magnification. Bone is outlined in blue. Calibration bar 500 μm.

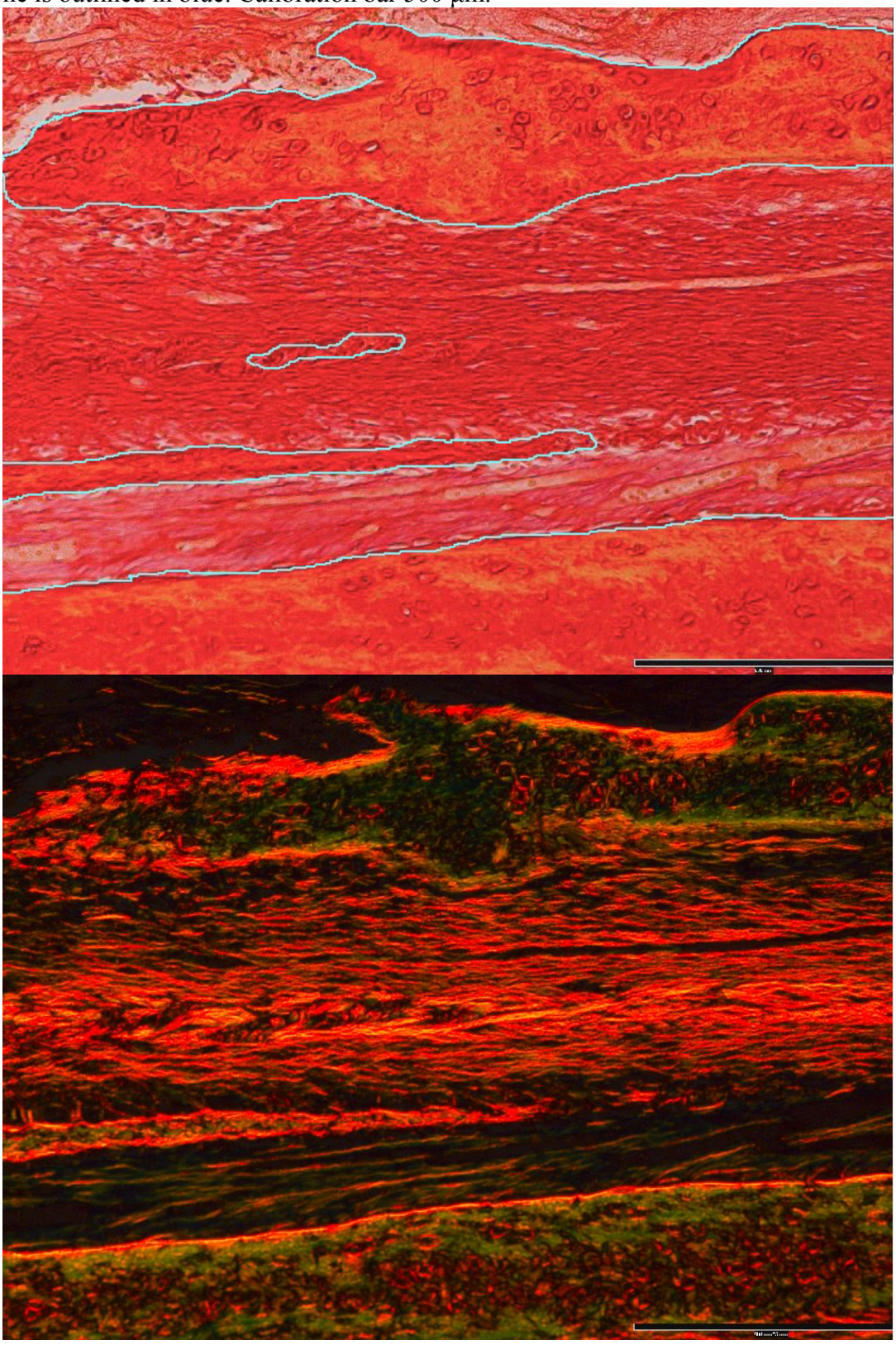

Figure 9: Average sutural width and S. D. comparing experimental and sham Yucatan minipigs.

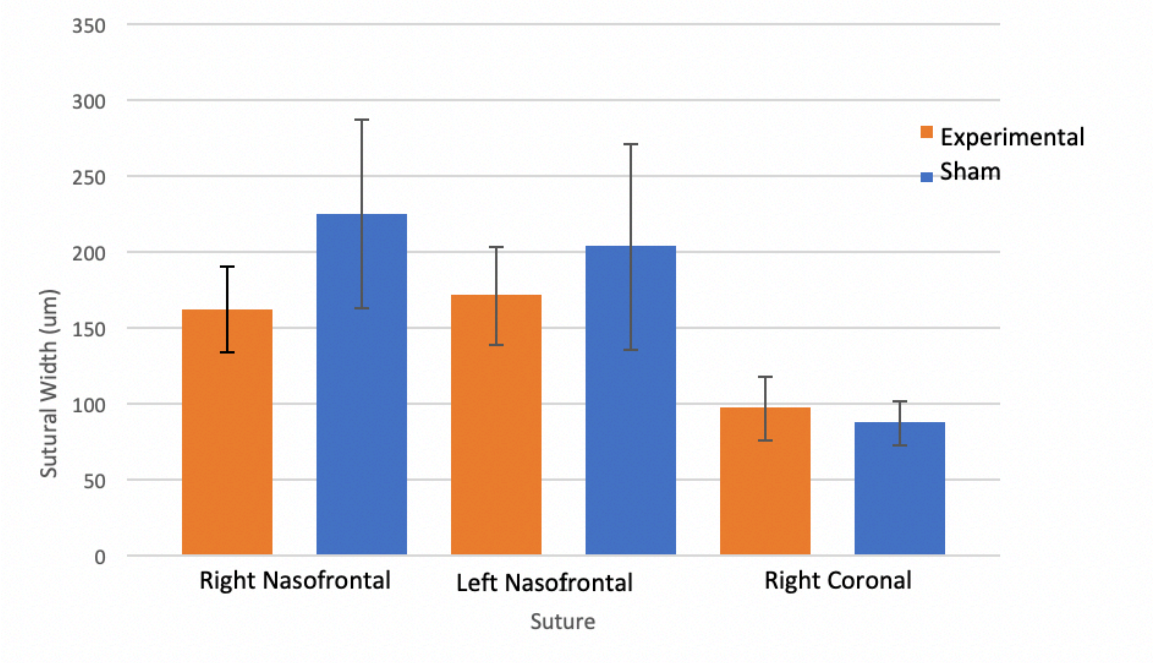

Figure 10: Average calcein width and S.D. for each suture of the experimental and sham Yucatan minipigs.

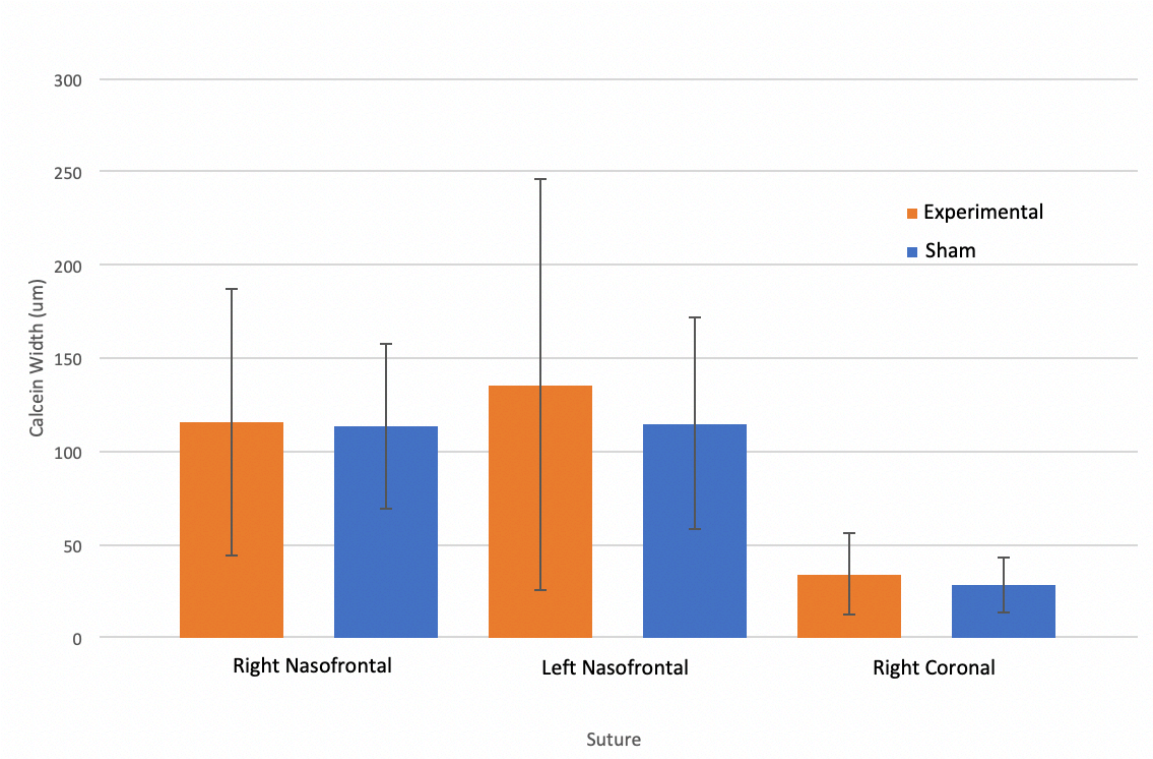

Figure 11: Average endothelial areal density (%) and S.D. for Yucatan minipigs and farm pigs. Right nasofrontal suture (RNFS), left nasofrontal suture (LNFS), right coronal suture (RCS).

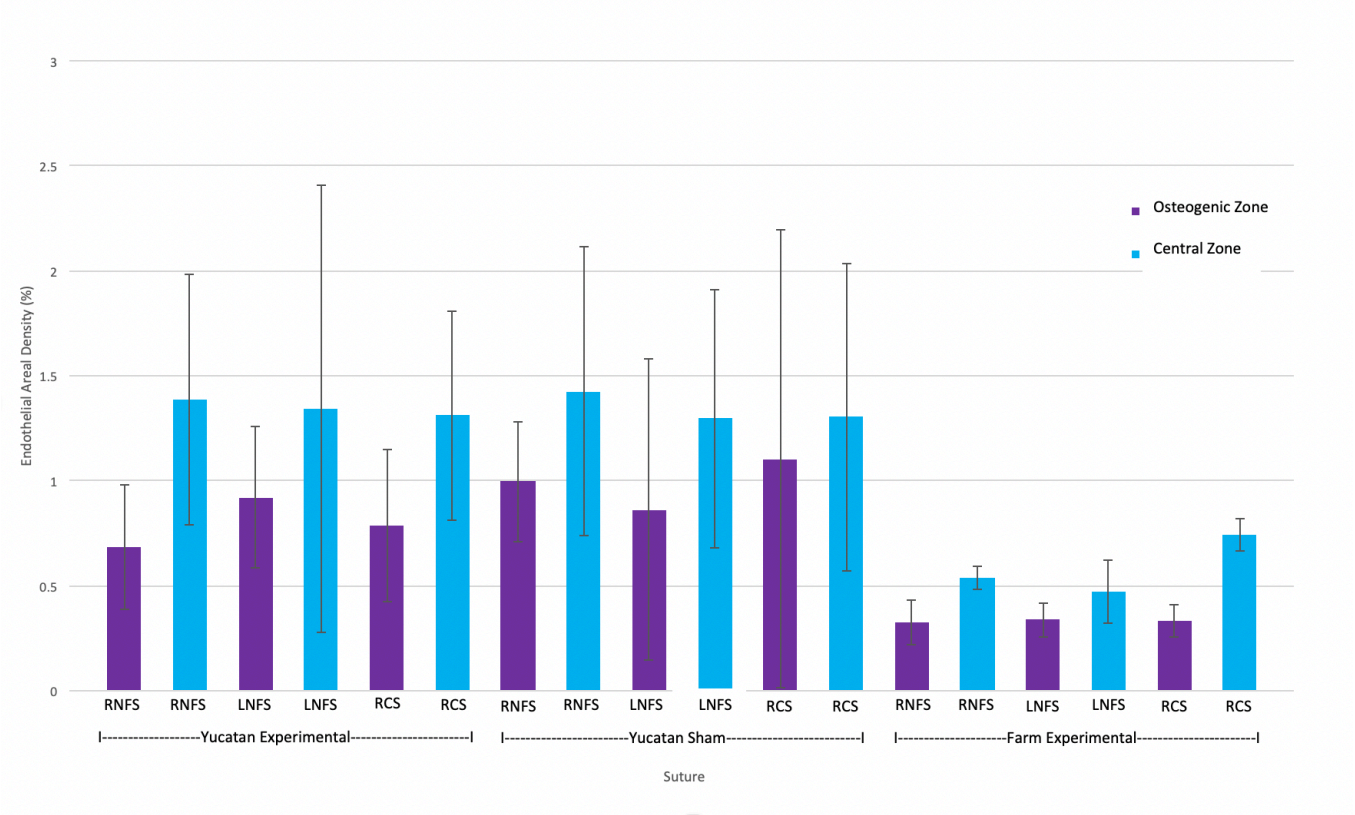

Figure 12: A. Dorsal section of a right nasofrontal suture of farm pig 594 (experimental). B. The comparable area from farm pig 595 (sham). Sirius red stain, polarized light. The circled area is the central zone of each suture. Calibration bar 500 μm.

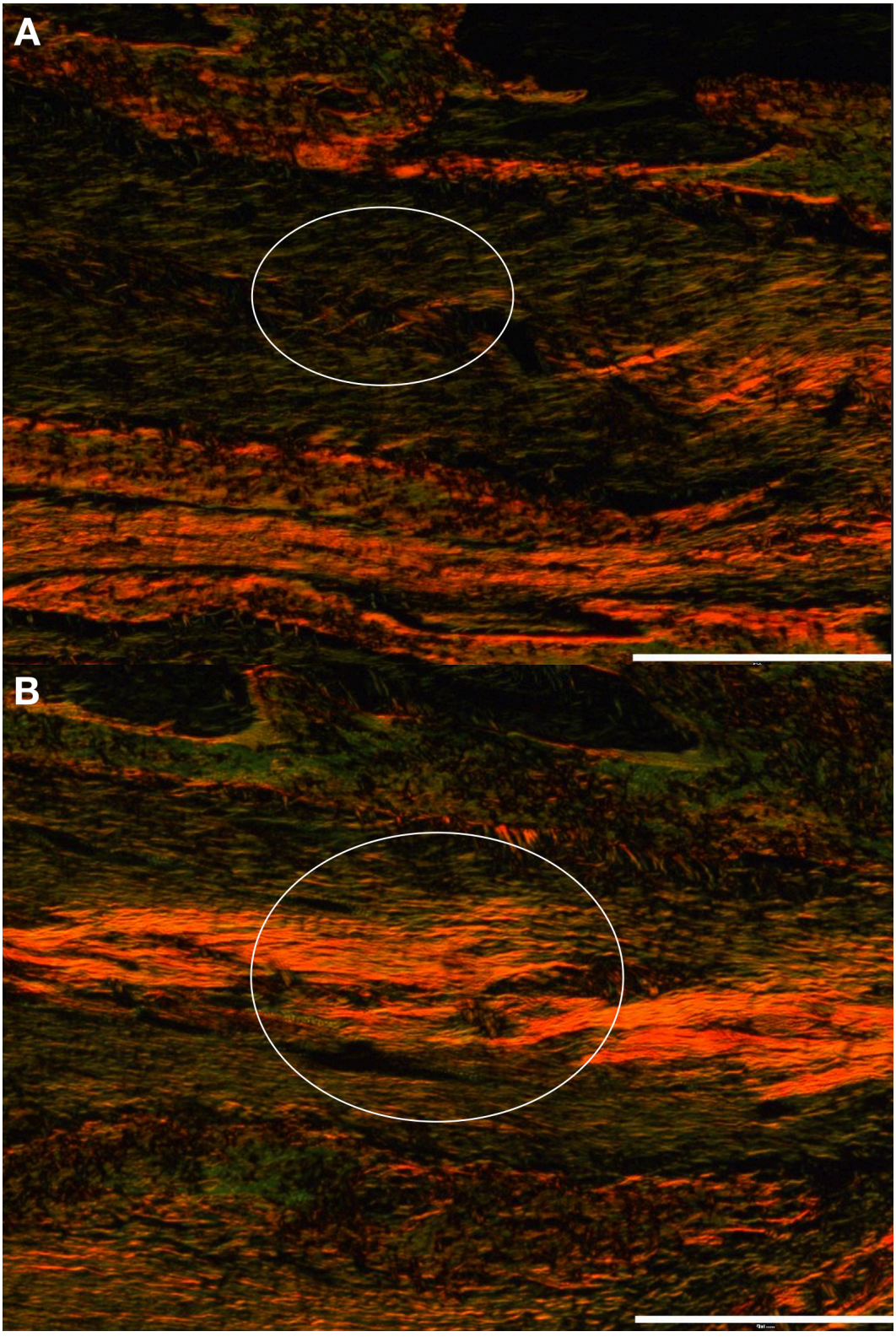

Figure 13: A. Right nasofrontal suture of Yucatan minipig 934 (experimental). B. Right nasofrontal suture of Yucatan minipig 938 (sham), middle section. Arrows pointing to attachment points. Circles show disorganized collagen fibers in A and uniform fibers in B. Calibration bar 500 μm.

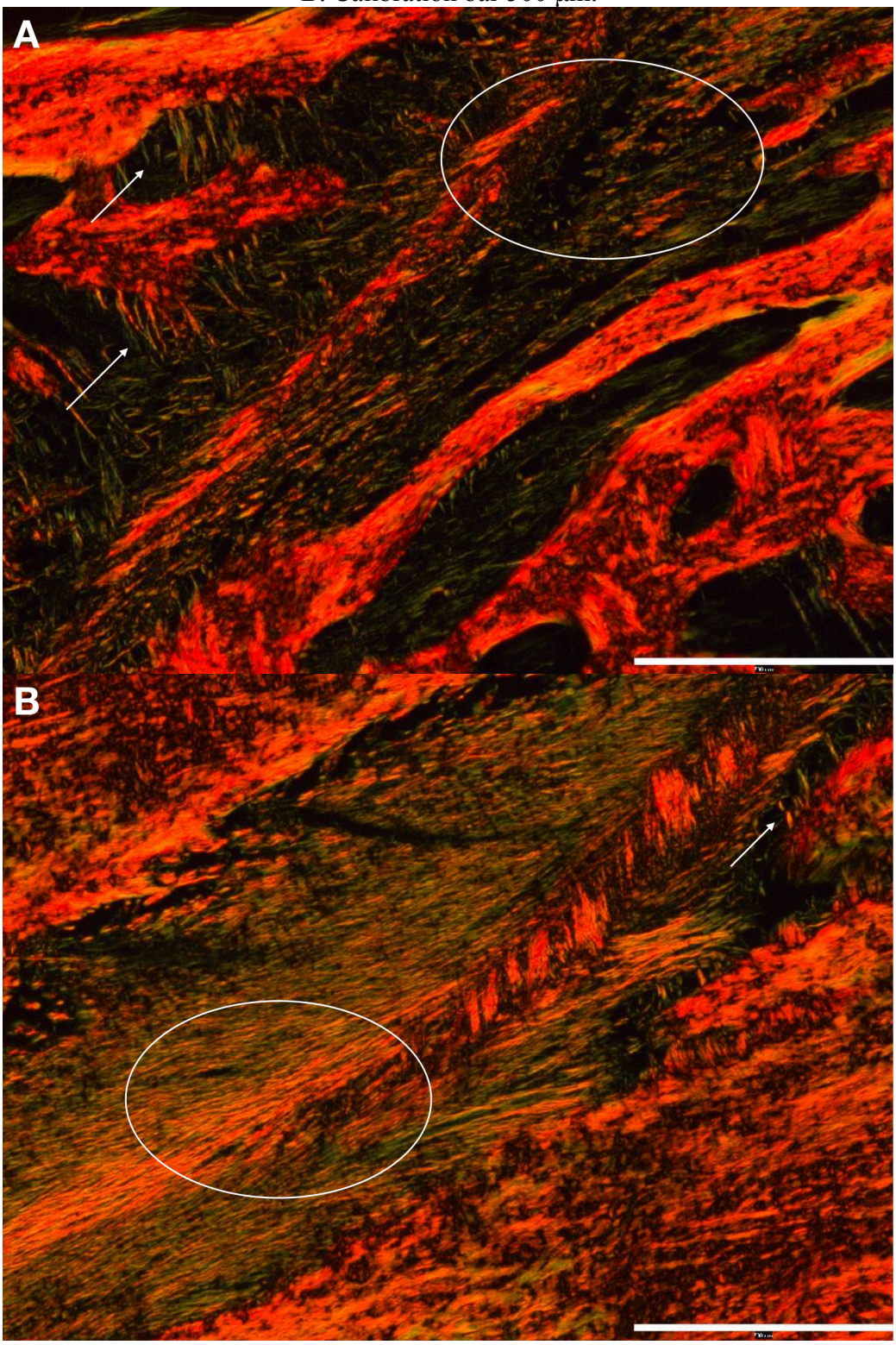

Figure 14: A. Left nasofrontal suture of Yucatan minipig 3351 (experimental). B. Left nasofrontal suture of Yucatan minipig 3355 (sham), dorsal section. Circles show disorganized collagen fibers in A and uniform fibers in B. Calibration bar 500 μm.